

Observations of laser induced magnetization dynamics in Co/Pd multilayers with coherent x-ray scattering

B. Wu,^{1,a)} D. Zhu,² Y. Acremann,³ T. A. Miller,⁴ A. M. Lindenberg,^{2,4} O. Hellwig,⁵ J. Stöhr,² and A. Scherz²

¹Department of Applied Physics, Stanford University, Stanford, California 94035, USA

²SLAC National Accelerator Laboratory, Menlo Park, California 94025, USA

³Laboratorium f. Festkörperphysik, ETH Zürich, 8093 Zürich, Switzerland

⁴Department of Material Science and Engineering, Stanford University, Stanford, California 94035, USA

⁵San Jose Research Center, Hitachi Global Storage Technologies, San Jose, California 95120, USA

(Received 10 October 2011; accepted 24 November 2011; published online 22 December 2011)

We report on time-resolved coherent x-ray scattering experiments of laser induced magnetization dynamics in Co/Pd multilayers with a high repetition rate optical pump x-ray probe setup. Starting from a multi-domain ground state, the magnetization is uniformly reduced after excitation by an intense 50 fs laser pulse. Using the normalized time correlation, we study the magnetization recovery on a picosecond timescale. The dynamic scattering intensity is separated into an elastic portion at length scales above 65 nm, which retains memory of the initial domain magnetization, and a fluctuating portion at smaller length scales corresponding to domain boundary motion during recovery. © 2011 American Institute of Physics. [doi:10.1063/1.3670305]

The magnetization of excited states define the operation processes and timescales in magnetic devices. The desire to explore the ultimate limits of magnetization dynamics, coupled with the explosive growth of information storage and communication technologies, has spurred the subsequent intense search for ways to manipulate and control magnetization on ever faster timescales and smaller length scales.¹⁻³ Operational bounds of technological devices are set by the timescale at which dynamic processes cease to be repeatable.⁴ To explore these limits therefore requires knowledge of the spatial and time correlation of excited states.

Recently, all-optical magnetization reversal, in which deterministic switching of the magnetization is achieved by a single 40 fs circularly polarized laser pulse, was demonstrated.^{5,6} Ultrafast laser spectroscopy has largely been driven by all-optical pump-probe techniques, which allow ultrafast excitations and the study of their evolution on the macroscopic scale by use of the magneto-optical Kerr or Faraday effect. However, little is known about the processes on the atomic to mesoscopic length scale because of the lack of spatial resolution of these techniques. Synchrotron-based techniques such as resonant magnetic scattering⁷ and coherent diffractive imaging^{8,9} can spatially resolve the magnetic correlations in a sample, but the flux limitations of time-resolved setups¹⁰ have prevented high resolution imaging with these techniques.

Here we demonstrate time-resolved coherent x-ray scattering at a synchrotron by utilizing a high repetition rate pump-probe setup.^{11,12} Using a 5.12 MHz repetition rate Ti:Sapphire laser phase locked to the revolution clock (1.28 MHz) of the Stanford synchrotron radiation lightsource (SSRL) operating in four bunch mode, we directly observe magnetization relaxation in Co/Pd multilayer samples with 50 ps time resolution out to momentum transfer

$q = 0.150 \text{ nm}^{-1}$. Coherent scattering further enables us to calculate the correlation between scatterings at different time delays and disentangle the origins of q -dependent scattering changes.

The sample consists of a $[\text{Co}(0.5 \text{ nm})\text{Pd}(0.7 \text{ nm})]_{15}$ multilayer thin film sputter deposited on a $200 \text{ by } 200 \mu\text{m}$ Si_3N_4 membrane at 3 mTorr Ar pressure. This sample has out-of-plane magnetization, forming worm domains of approximately 100 nm in width, as shown in the MAD Holography reconstruction¹³ in Fig. 1(a). Striped domain phases with perpendicular magnetization are well established magnetic systems with strong scattering cross sections.^{14,15} Quasi-static magnetization changes in an external field have been studied in these systems,¹⁶ but the response to laser excitation remains unexplored.

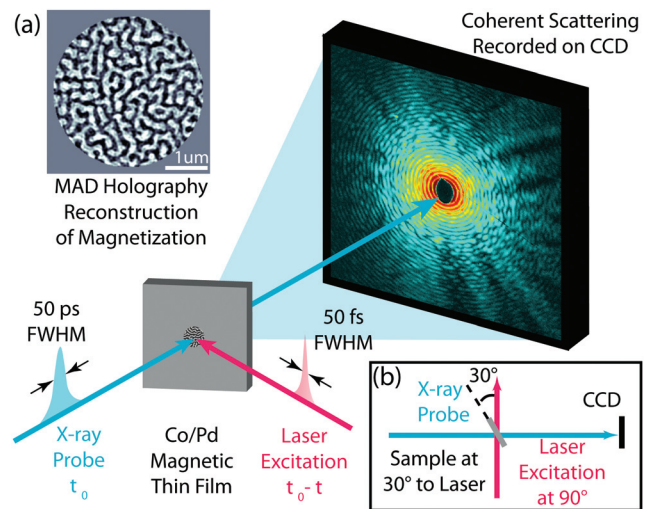


FIG. 1. (Color) Schematic of optical pump x-ray probe experimental setup. (a) Sample magnetization reconstructed using MAD Holography.¹³ (b) Overhead schematic of experimental geometry.

^{a)}Electronic mail: bennywu@stanford.edu.

A schematic of the experimental setup is shown in Fig. 1, with the overhead geometry in Fig. 1(b). The system is excited by a 50 fs optical pump pulse from a long cavity Ti:Sapphire laser at 800 nm, then probed after a variable delay t with a circularly polarized coherent x-ray pulse at the Co L3 edge of approximately 50 ps FWHM. The time-resolved small angle diffraction pattern is captured with a Princeton Instruments MTE1340 soft x-ray CCD detector. Using the highest laser fluence available, the pump laser is focused to a spot size of less than 20 by 20 μm , corresponding to a fluence of approximately 5 mJ/cm² at the sample. The x-ray probe size is approximately 220 by 70 μm . To confine the probe size, 800 nm of Au is first deposited on the back side of the sample, then a 3 μm aperture is milled with a focused ion beam as described in Ref. 8. The opaque gold mask ensures that the x-rays probe an area with uniform laser fluence and facilitates heat dissipation from the high repetition rate pump laser. We obtained a coherent flux of 2×10^6 photons/ μm^2 /s or 10% of the flux under normal operations. For each time delay, both the pump probe and the reference images are accumulations over 240 s.

Scattered x-rays from the magnetic domains in the sample create a speckle pattern reflecting the exact spatial arrangement of the magnetic domains.^{7,17} The scattering intensity is a combination of the magnetic and charge scattering contributions from the domains and the aperture, respectively, and is given by $I(t) = |c|^2 + |m(t)|^2 + 2|c||m(t)|\cos\Delta\phi$. Here c represents the charge scattering, $m(t)$ the time-dependent magnetic scattering, and $\Delta\phi$ the phase of the charge-magnetic interference. Changes in the scattering can be calculated by comparing patterns from the pumped sample at time delays of interest, $t = -40$ ps to +3 ns, to a reference pattern from the unperturbed sample at negative time delay, $t_{\text{ref}} = -1$ ns. This procedure allows for removal of the *time-independent* charge scattering $|c|^2$ in the raw data (Fig. 1) for all time delays as shown in Fig. 2(a). Since $|m|/|c| \ll 1$ (Ref. 18), the normalized difference in magnetic scattering intensity is in good approximation

$$\Delta I_{\text{norm}} = \frac{I(t_{\text{ref}}) - I(t)}{I(t_{\text{ref}}) + I(t)} = \frac{\Delta m(t) \cos \Delta\phi}{|c|}. \quad (1)$$

This relation holds when the overall magnetization $\Delta m(t) = |m_s| - |m(t)|$ changes in the domains while their arrangement is maintained ($\Delta\phi = \text{const}$).

Normalized diffraction patterns ΔI_{norm} for given time delays are shown in Fig. 2(a). Reduction of the out-of-plane component magnetization during demagnetization leads to a negative background in the normalized difference. The continued presence of speckles in a given q range indicates that the domain configuration is maintained during the exposure. Therefore, we can apply Eq. (1) and normalize $\Delta m(t)\cos\Delta\phi/|c|$ to $m_s\cos\Delta\phi/|c|$ deduced from static speckle patterns.^{17,19} The resulting demagnetization curve is shown in Fig. 2(b). There is a clear build up in the normalized difference signal, with the maximum signal seen at +60 ps. The difference then decreases as the magnetization recovers.

Average magnitude of the normalized difference for different time delays as a function of q is shown in Fig. 3(a). The signal is strongest near 100 nm, corresponding to mag-

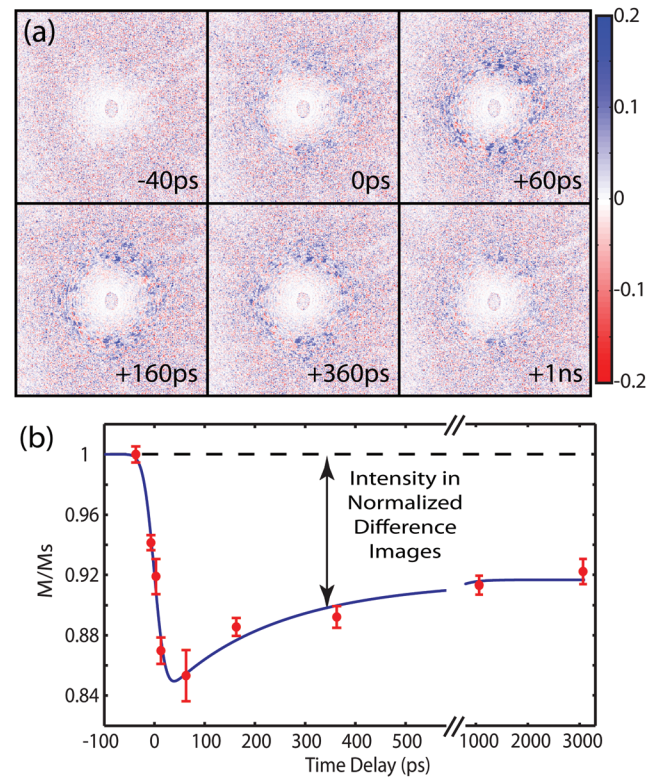


FIG. 2. (Color) (a) Normalized change in magnetic scattering at various time delays. The q range extends out to 0.125 nm^{-1} . The stable speckle configuration indicates that the underlying domain structure is maintained. (b) Demagnetization curve from ΔI_{norm} , which is proportional to deviation from $M/M_s = 1$. The line is a fit to the data with Koopman's micro three temperature model,²⁰ which indicates a demagnetization of 20%–25%. The plotted curve is significantly broadened by convolution with a 50 ps FWHM Gaussian corresponding to the width of the x-ray probe.

netization reduction within the domains following the initial excitation. The nature of coherent scattering makes it possible to determine the relative size of the repeatable and non-repeatable portions of the dynamics. We calculate the normalized time correlation function

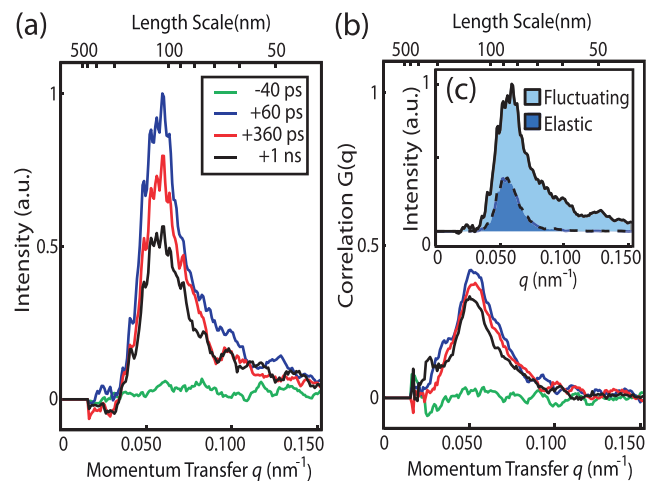


FIG. 3. (Color) (a) Radial integration of the normalized difference for different time delays. (b) Corresponding q dependent correlation to the normalized difference at 0 ps. (c) Shown for the +60 ps signal, by multiplying panels a and b, the elastic and fluctuating portions of the magnetization changes can be identified.

$$G(t, q) = \frac{I'_{t=0}(q) \cdot I'_t(q)}{\|I'_{t=0}(q)\| \|I'_t(q)\|}, \quad (2)$$

where $I'_n(q) = I_n(q) - \langle I_n(q) \rangle$ and $I_n(q)$ consists of the measured intensities within an annulus 5 pixels wide centered with respect to the diffraction pattern and stepped across in steps of one pixel.²¹ As shown in Fig. 3(b), the time correlation is centered around the magnetic scattering peak, and drops to zero for length scales below 65 nm. This suggests that after optical excitation, memory of the initial domain magnetization is retained in a low q portion of the sample. By multiplying the time correlation and radial integration signals together, we can identify the correlated, elastic portion of the scattering. The remaining scattering is then attributed to a fluctuating portion as shown in Fig. 3(c). The presence of a small elastic component indicates that the pump fluence is in a borderline regime where irreversible changes of the domain structure are emerging. During recovery, as hot electrons scatter off domain walls, angular momentum transfer leads to fluctuations of the magnetic order and motion of the magnetic domain boundaries. These fluctuations lead to a progressive loss of correlation for length scales below 65 nm.

In conclusion, we have demonstrated time resolved coherent x-ray scattering experiments at a synchrotron. Picosecond time-resolved diffraction data taken on Co/Pd multilayer samples show that after excitation by a femtosecond optical pulse, the magnetic contrast is sharply reduced, followed by a slow magnetization recovery over a nanosecond timescale. The speckle pattern remains stable during the recovery, indicating that the spatial arrangement of magnetic domains in the sample is maintained. The normalized time correlation is used to separate the dynamic scattering intensity into an elastic portion at low q , corresponding to a disordering of spins within the individual domains which retains the initial domain structure, and a fluctuating portion at high q attributed to motions of magnetic domain boundaries during relaxation.

Picosecond time resolved coherent scattering experiments at 3rd generation synchrotron sources will enable the study of many dynamic processes, including the determination of technological switching limits. Of special interest to the magnetism community is all-optical switching, which occurs on picosecond time scales.⁶ In the future, time-resolved laser pump x-ray probe experiments at X-ray Free Electron Laser (XFEL) facilities, such as the Linear Coherent Lightsource, will provide access to sub-picosecond dynamics with both femtosecond temporal resolution and nanometers spatial resolution. Additional opportunities for carrying out measurements with few picosecond time-resolution at SSRL will be possible with low alpha timing modes.²² Time-resolved coherent scattering experiments at 3rd generation synchrotrons will thus complement experiments at XFELs, allowing a wide range of dynamics to be

probed with nanometer scale resolution over the femtosecond to nanosecond time scale.

The authors are grateful to H. Dürr for fruitful discussions and to J. Safranek and W. Corbett for support during Accelerator Physics shifts at SSRL. This research is supported through the PULSE and SIMES Institutes at SLAC/Stanford by the U.S. Department of Energy, Office of Basic Energy Sciences, and by SLAC LDRD funding.

¹E. Beaurepaire, J. C. Merle, A. Daunois, and J. Y. Bigot, *Phys. Rev. Lett.* **76**, 4250 (1996).

²B. Koopmans, J. J. M. Ruigrok, F. Dalla Longa, and W. J. M. de Jong, *Phys. Rev. Lett.* **95**, 267207 (2005).

³M. Cinchetti, M. S. Albaneda, D. Hoffmann, T. Roth, J. P. Wustenberg, M. Krauss, O. Andreyev, H. C. Schneider, M. Bauer, and M. Aeschlimann, *Phys. Rev. Lett.* **97**, 177201 (2006).

⁴I. Tudosa, C. Stamm, A. B. Kashuba, F. King, H. C. Siegmann, J. Stöhr, G. Ju, B. Lu, and D. Weller, *Nature* **428**, 831 (2004).

⁵C. Stanciu, F. Hansteen, A. V. Kimel, A. Kirilyuk, A. Tsukamoto, A. Itoh, and Th. Rasing, *Phys. Rev. Lett.* **99**, 047601 (2007).

⁶K. Vahaplar, A. M. Kalashnikova, A. V. Kimel, D. Hinzke, U. Nowak, R. Chantrell, A. Tsukamoto, A. Itoh, A. Kirilyuk, and Th. Rasing, *Phys. Rev. Lett.* **103**, 117201 (2009).

⁷J. P. Hannon, G. T. Trammell, M. Blume, and D. Gibbs, *Phys. Rev. Lett.* **61**, 1245 (1988).

⁸S. Eisebitt, J. Luning, W. F. Schlotter, M. Lorgen, O. Hellwig, W. Eberhardt, and J. Stöhr, *Nature* **432**, 885 (2004).

⁹A. Scherz, W. F. Schlotter, K. Chen, R. Rick, J. Stöhr, J. Luning, I. McNulty, C. M. Gunther, F. Radu, W. Eberhardt, O. Hellwig, and S. Eisebitt, *Phys. Rev. B* **76**, 214410 (2007).

¹⁰R. W. Schoenlein, S. Chattopadhyay, H. H. W. Chong, T. E. Glover, P. A. Heimann, C. V. Shank, A. A. Zholents, M. S. Zolotarev, *Science* **287**, 2237 (2000).

¹¹F. A. Lima, C. J. Milne, D. C. V. Amarasinghe, M. H. Rittmann-Frank, R. M. van der Veen, M. Reinhard, V. T. Pham, S. Karlsson, S. L. Johnson, D. Grolimund, C. Borca, T. Huthwelker, M. Janousch, F. van Mourik, R. Abela, and M. Chergui, *Rev. Sci. Instrum.* **82**, 063111 (2011).

¹²A. M. March, A. Stickrath, G. Doumy, E. P. Kanter, B. Krässig, S. H. Southworth, K. Attenkofer, C. A. Kurtz, L. X. Chen, and L. Young, *Rev. Sci. Instrum.* **82**, 073110 (2011).

¹³T. Wang, R. Rick, D. Zhu, B. Wu, O. Hellwig, J. Stöhr, and A. Scherz, "Imaging dichroic materials with multi-wavelength anomalous diffraction" (unpublished).

¹⁴M. S. Pierce, R. G. Moore, L. B. Sorensen, S. D. Kevan, O. Hellwig, E. E. Fullerton, and J. B. Kortright, *Phys. Rev. Lett.* **90**, 175502 (2003).

¹⁵O. Hellwig, A. Berger, J. B. Kortright, and E. E. Fullerton, *J. Magn. Magn. Mater.* **319**, 13 (2007).

¹⁶O. Hellwig, G. P. Denbeaux, J. B. Kortright, and E. E. Fullerton, *Physica B* **336**, 136 (2003).

¹⁷S. Eisebitt, M. Lörger, W. Eberhardt, J. Luning, J. Stöhr, C. T. Rettner, O. Hellwig, E. E. Fullerton, and G. Denbeaux, *Phys. Rev. B* **68**, 104419 (2003).

¹⁸M. Blume, *J. App. Phys.* **57**, 3615 (1985).

¹⁹ $(I_+ - I_-)/(I_+ + I_-) = 2m_s \cos \Delta\phi / |c|$ for speckle patterns recorded with left(-) and right(+) circularly polarized x-rays.

²⁰B. Koopmans, G. Malinowski, F. D. Longa, D. Steiauf, M. Fahnle, T. Roth, M. Cinchetti, and M. Aeschlimann, *Nat. Mater.* **9**, 259 (2010).

²¹A. Barty, S. Boutet, M. Bogan, S. Hau-Riege, S. Marchesini, K. Sokolowski-Tinten, N. Stojanovic, R. Tobey, H. Ehrke, A. Cavalleri, S. Dusterer, M. Frank, S. Bajt, B. Woods, M. Seibert, J. Hajdu, R. Treusch, and H. Chapman, *Nat. Photonics* **2**, 415 (2008).

²²T. A. Miller, J. Corbett, J. Wittenberg, D. Daranciang, J. Goodfellow, A. S. Fisher, X. Huang, W. Mok, J. Safranek, H. Wen, and A. Lindenberg, in Proceedings of IPAC'10, WEOCMH03, Kyoto, Japan, 23–28 May 2010.